

## Recent Results from Investigations of Diffractive Vector Meson Production with the ZEUS Detector at HERA

J.A. Crittenden

*Physikalisches Institut, Universität Bonn, Nußallee 12, 53115 Bonn, Germany*  
on behalf of the ZEUS collaboration

We present results from recent investigations of diffractive vector meson production using the ZEUS detector at HERA. These consist of measurements of  $\rho^0$  production in the region of photon virtuality  $0.25 < Q^2 < 0.85 \text{ GeV}^2$ , of  $\rho^0$ ,  $\phi$ , and  $J/\psi$  production for values of the momentum transfer to the proton  $0.3 < |t| < 4.0 \text{ GeV}^2$ , and of elastic  $J/\psi$  production both in photoproduction and for  $Q^2 > 2 \text{ GeV}^2$ .

### 1 Introduction

The subject of elastic vector meson production at high energies has attracted much attention due to its contributions to the new field of hard diffraction. Such measurements of *exclusive* processes, a rarity at high-energy colliders, represent a new opportunity to test calculations within the framework of perturbative quantum chromodynamics (pQCD).<sup>1</sup> Here we present recent measurements of diffractive vector meson production with the ZEUS experiment in the interactions of 27.5 GeV positrons with 820 GeV protons at HERA. Further details may be found in papers submitted to the recent DIS '97 Workshop<sup>2</sup>. We concentrate on three topics:

- elastic production of  $\rho^0$  mesons in an intermediate range of photon virtuality  $Q^2$ ,  $0.25 < Q^2 < 0.85 \text{ GeV}^2$ . This analysis is based on measurements recorded using a special-purpose electromagnetic calorimeter with acceptance at positron scattering angles between 17 and 35 mrad, called the beam-pipe calorimeter (BPC),
- photoproduction of  $\rho^0$ ,  $\phi$ , and  $J/\psi$  mesons for high absolute values of the squared momentum transferred to the proton,  $|t|$ ,  $0.3 < |t| < 4.0 \text{ GeV}^2$ . Since the final-state proton system (usually dissociated) was not detected, its transverse momentum was approximated by the transverse momentum of the final-state vector meson. The difference is kinematically limited to a value less than  $Q^2$ . Detection of the final-state positron in another special-purpose calorimeter 44 m distant from the interaction point ("44-meter tagger"), limited  $Q^2$  to values less than  $0.01 \text{ GeV}^2$ , ensuring the validity of the approximation at that level,
- production of  $J/\psi$  mesons both for untagged photoproduction ( $10^{-10} <$

$Q^2 < 4 \text{ GeV}^2$ ), and for a sample where the final-state positron was detected in the central calorimeter ( $Q^2 > 2 \text{ GeV}^2$ ).

Central to these investigations is the question of the validity of pQCD calculations, an issue which has stimulated much interest due in part to the novelty of applying perturbative methods to diffractive processes.<sup>3</sup> It has been suggested that the necessary hard scale may be given by  $Q^2$ ,  $t$ , or the vector-meson mass. Our investigations aim to test these ideas.

## 2 Elastic Electroproduction of $\rho^0$ Mesons

The exclusive dipion BPC sample recorded in 1995 with an integrated luminosity of  $3.8 \text{ pb}^{-1}$  includes about 6000 events in the  $\rho^0$  mass region and covers the kinematic range  $0.25 < Q^2 < 0.85 \text{ GeV}^2$ ,  $|t| < 0.6 \text{ GeV}^2$ ,  $20 < W_{\gamma^*p} < 90 \text{ GeV}$ , where  $W_{\gamma^*p}$  is the center-of-mass energy of the virtual-photon-proton system. The invariant mass spectrum in the  $\rho^0$  mass region is shown in Fig. 1, together with the results of a fit to the squared coherent sum of a Breit–Wigner resonance term and a nonresonant background term:

$$\frac{dN}{dM_{\pi\pi}} = \left| A \frac{\sqrt{M_{\pi\pi} M_\rho \Gamma_\rho}}{M_{\pi\pi}^2 - M_\rho^2 + i M_\rho \Gamma_\rho} + B \right|^2. \quad (1)$$

The dashed line on the mass spectrum indicates the sum of the contributions

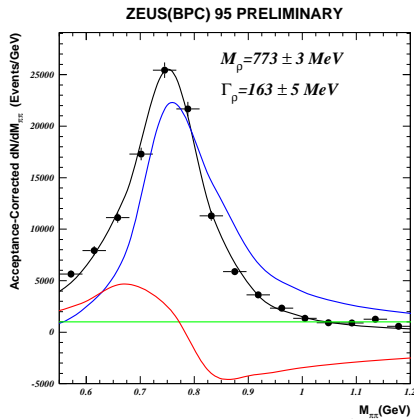


Figure 1: Acceptance-corrected  $\pi^+\pi^-$  invariant mass distribution for elastic  $\rho^0$  production at intermediate  $Q^2$

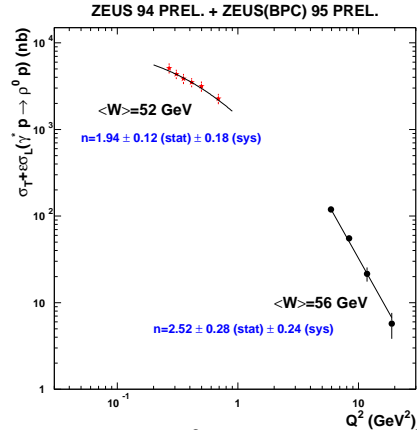


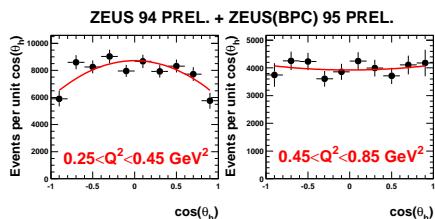
Figure 2: The  $Q^2$  dependence of the  $\rho^0$  elastic cross section

from the Breit–Wigner resonance term (*dotted line*), the nonresonant background term (*dash-dotted line*), and the interference term (*solid line*). The resonant cross section averaged over  $W_{\gamma^*p}$  is plotted as a function of  $Q^2$  in Fig. 2 and compared to the measurements<sup>4</sup> at similar  $W_{\gamma^*p}$  and high  $Q^2$  in order to investigate the  $Q^2$  dependence. The result of a fit to the dependence  $(Q^2 + M_\rho^2)^{-n}$  yields the result  $n = 1.94 \pm 0.12(\text{stat}) \pm 0.18(\text{sys})$ , consistent with pQCD calculations for longitudinal photons. However, the cross sections measured here are the sum of contributions from longitudinal and transverse photons  $\sigma_L + \varepsilon\sigma_T$ , where  $\varepsilon$  is the ratio of the transverse to longitudinal photon flux ( $0.97 < \varepsilon < 1.00$ ). This ambiguity in the comparison to the calculations will be removed when information on the ratio  $R = \sigma_L/\sigma_T$  becomes available.

A first attempt to measure this ratio is exemplified in Figs. 3 and 4. Figure 3 shows the polar angle distribution of the  $\pi^+$  direction in the  $\rho^0$  rest system with the  $Z$  axis defined as the direction opposite to the final-state proton momentum. This distribution depends on the spin-density matrix element  $r_{00}^{04}$  (the probability that the  $\rho^0$  is produced with longitudinal polarization<sup>5</sup>):

$$\frac{1}{N} \frac{dN}{d(\cos\theta_h)} = \frac{3}{4} [1 - r_{00}^{04} + (3r_{00}^{04} - 1) \cos^2\theta_h]. \quad (2)$$

The distributions indicate that the BPC data cover a region of transition to increasingly longitudinal polarization at high  $Q^2$ . Assuming that the  $s$ -channel



$Q^2$ (GeV <sup>2</sup> )	$r_{00}^{04}$
0.34	$0.24 \pm 0.02(\text{stat})$
0.62	$0.34 \pm 0.03(\text{stat})$
5.8	$0.71^{+0.03}_{-0.04}(\text{stat})^{+0.01}_{-0.01}(\text{sys})$
8.2	$0.76^{+0.04}_{-0.04}(\text{stat})^{+0.00}_{-0.02}(\text{sys})$
14	$0.79^{+0.04}_{-0.05}(\text{stat})^{+0.02}_{-0.01}(\text{sys})$

Figure 3: Polar decay angle distributions for the BPC  $\rho^0$  samples and fit results for  $r_{00}^{04}$  at intermediate and high  $Q^2$

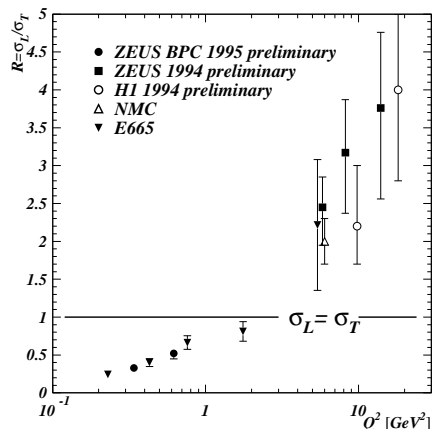


Figure 4: Values for  $R$  as a function of  $Q^2$  derived from the spin-density matrix element  $r_{00}^{04}$  under the assumption of SCHC

helicity conservation (SCHC) observed at low energy holds at HERA energies,

the ratio  $R$  is related to this matrix element as  $R = r_{00}^{04}/\varepsilon(1 - r_{00}^{04})$ . Figure 4 shows the corresponding  $R$  values, comparing them to the ZEUS results<sup>4</sup> at high  $Q^2$ , those from H1,<sup>6</sup> and those from fixed target muoproduction.<sup>7</sup> The need for this assumption will remain until full helicity analyses are available.

### 3 Elastic $\rho^0$ , $\phi$ , and $J/\psi$ Photoproduction at High $|t|$

The ZEUS collaboration has presented<sup>8</sup> a sample of about 80000 untagged elastic photoproduced  $\rho^0$  meson events based on  $2.2 \text{ pb}^{-1}$  recorded in 1994, covering the kinematic range  $10^{-10} < Q^2 < 4 \text{ GeV}^2$ ,  $\langle Q^2 \rangle \simeq 10^{-2} \text{ GeV}^2$ ,  $|t| < 0.5 \text{ GeV}^2$ , and  $50 < W_{\gamma^*p} < 100 \text{ GeV}$ . The statistical accuracy of this sample allowed the determination of the relative contributions from resonant and nonresonant dipion production as a function of  $t$  (eq. 1). The new analysis of about 30000 events from an integrated luminosity of  $2.1 \text{ pb}^{-1}$  recorded with the 44-m tagger in 1995 ( $10^{-9} < Q^2 < 0.01 \text{ GeV}^2$ ,  $\langle Q^2 \rangle \simeq 10^{-3} \text{ GeV}^2$ ,  $|t| < 4.0 \text{ GeV}^2$ , and  $85 < W_{\gamma^*p} < 105 \text{ GeV}$ ) allows the extension of this study to higher  $|t|$ , as shown in Fig. 5. At values of  $|t|$  exceeding  $1 \text{ GeV}^2$  the

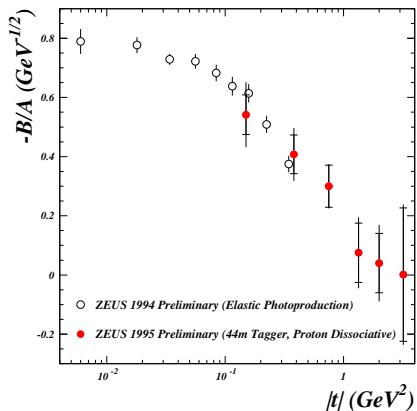


Figure 5: Ratio of dipion mass spectrum fit parameters,  $B/A$ , as a function of  $t$  (eq. 1)

measurements are consistent with no nonresonant background contribution. The smooth transition and the fact that the high  $|t|$  data are dominated by proton dissociative processes indicate that the pion pair production proceeds independently of the proton dissociation.

Clean  $\phi$  and  $J/\psi$  signals have also been observed in the 44-m tagger sample, allowing the investigation of production ratios relative to the  $\rho^0$  as a function

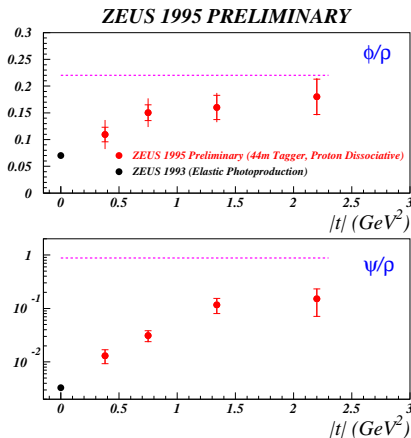


Figure 6: Ratios of  $\phi$  and  $J/\psi$  production to  $\rho^0$  production as a function of  $t$

of  $|t|$ , shown in Fig. 6. At high  $|t|$  the ratios approach values derived from simple quark-counting rules and flavor-independent production which result in the expectation for the ratios:  $\rho^0 : \phi : J/\psi = 9 : 2 : 8$ .

#### 4 Photo- and Electroproduction of $J/\psi$ Mesons

Photoproduction of  $J/\psi$  mesons for  $10^{-10} < Q^2 < 4 \text{ GeV}^2$ ,  $\langle Q^2 \rangle \simeq 10^{-1} \text{ GeV}^2$ , and  $40 < W_{\gamma^*p} < 140 \text{ GeV}$  has been investigated<sup>9</sup> via their leptonic decays. An integrated luminosity of  $2.70 \text{ pb}^{-1}$  ( $1.87 \text{ pb}^{-1}$ ) from 1994 was analyzed for the  $e^+e^-$  ( $\mu^+\mu^-$ ) decay mode, yielding  $460 \pm 25$  ( $266 \pm 17$ ) events. A fit to the dependence  $W_{\gamma^*p}^\delta$  yields the result  $\delta = 0.92 \pm 0.14(\text{stat}) \pm 0.10(\text{sys})$ , inconsistent with the exchange of a soft Pomeron alone ( $\delta \simeq 0.22$ ).<sup>10</sup> Figure 7 shows the extraction of the  $|t|$  dependence in  $J/\psi$  photoproduction: (a) the dependence of the  $J/\psi$  photoproduction cross section on the squared transverse momentum of the  $J/\psi$ ,  $p_{T\psi}^2$ , (b) the factor,  $F$ , required to relate the  $p_{T\psi}^2$  dependence to the  $|t|$  dependence, derived from simulations, (c) the  $|t|$ -dependence of the  $J/\psi$  elastic photoproduction cross section. The fit to the function  $e^{-b|t|}$  yields  $b =$

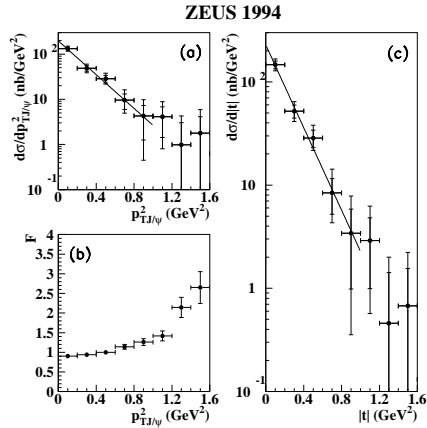


Figure 7:  $p_{T\psi}^2$  and  $|t|$  dependence of the  $J/\psi$  elastic photoproduction cross section.

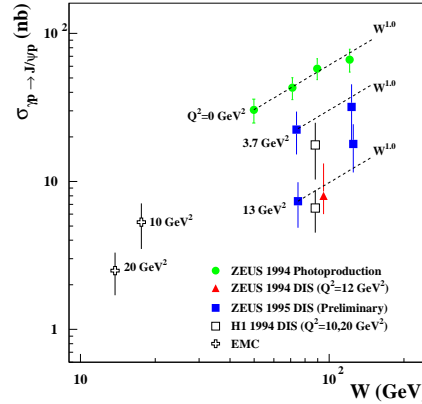


Figure 8: Energy dependence of the  $J/\psi$  electroproduction cross section

$4.6 \pm 0.4(\text{stat})_{-0.6}^{+0.4}(\text{sys}) \text{ GeV}^{-2}$ , indicating that the interaction radius is much smaller than that found<sup>11</sup> for the  $\rho^0$  ( $b = 9.8 \pm 0.8(\text{stat}) \pm 1.1(\text{sys}) \text{ GeV}^{-2}$ ).

An analysis of  $6 \text{ pb}^{-1}$  recorded in 1995 has allowed a measurement of the  $W_{\gamma^*p}$  dependence of the  $J/\psi$  electroproduction cross section for  $2 < Q^2 < 40 \text{ GeV}^2$  and  $50 < W_{\gamma^*p} < 150 \text{ GeV}$ , shown in Fig. 8. A fit to the dilepton mass signal region yields a signal of  $101 \pm 13$  events ( $e^+e^-$  and  $\mu^+\mu^-$  combined).

The  $t$ -slope is found to be  $b = 4.5 \pm 0.8$  (stat)  $\pm 1.0$  (sys)  $\text{GeV}^{-2}$ , consistent with the photoproduction result.

## 5 Summary

Analyses of the  $Q^2$  dependence of elastic  $\rho^0$  electroproduction, of  $\rho^0$  photoproduction at high values of the momentum transferred to the target proton, and of the energy dependence in  $J/\psi$  photoproduction lend credibility to the idea that the variables  $Q^2$ ,  $t$ , and  $M_V$  each can be used to define a transition region between soft and hard diffraction. The ZEUS experiment is sensitive to the transition region in *each* of these variables, allowing detailed, multi-parameter, studies of the transition from nonperturbative to perturbative QCD. The studies are statistics-limited and their precision is expected to improve dramatically when the more recent data sets have been analyzed.

## References

1. For a review of HERA results, see J.A.Crittenden, DESY Report 97-068 (1997), to appear as Nr. 140 in *Springer Tracts in Modern Physics*
2. Talks by L. Adamczyk, L. Bellagamba, and T. Monteiro at the 5th International Workshop on Deep Inelastic Scattering and QCD, April, 1997
3. M.G. Ryskin, *Z. Phys.* **C 57** (1993) 89; M.G. Ryskin *et al.*, Preprint HEP-PH/95-11-228 (1995); S.J. Brodsky *et al.*, *Phys. Rev.* **D 50** (1994) 3134; L. Frankfurt *et al.*, *Phys. Rev.* **D 54** (1996) 3194; A. Martin *et al.*, Preprint HEP-PH/96-09-448 (1996); J. Nemchik *et al.*, *Phys. Lett.* **374** (1996) 199; D.Yu. Ivanov, *Phys. Rev.* **D 53** (1996) 3564; I.F. Ginzburg and D.Yu. Ivanov, *Phys. Rev.* **D 54** (1996) 5523; J.R. Forshaw *et al.*, *Z. Phys.* **C 68** (1995) 137
4. The ZEUS Collaboration, PA02-028, XXVIII International Conference on High Energy Physics, Warsaw, Poland, July 25-31, 1996
5. K. Schilling and G. Wolf, *Nucl. Phys.* **B 61** (1973) 381
6. The H1 Collaboration, PA03-048, XXVIII International Conference on High Energy Physics, Warsaw, Poland, July 25-31, 1996
7. The NMC Collaboration, *Nucl. Phys.* **B 429** (1994) 503; The E665 Collaboration, *Z. Phys.* **C 72** (1997) 237
8. The ZEUS Collaboration, PA02-050, XXVIII International Conference on High Energy Physics, Warsaw, Poland, July 25-31, 1996
9. The ZEUS Collaboration, DESY Report 97-060 (1997)
10. M. Arneodo, these Proceedings
11. The ZEUS Collaboration, *Z. Phys.* **C 73** (1997) 253